REPORT DOCUMENTATION PAGE

Form Approved
OMB NO. 0704-0188

1. AGENCY USE ONLY (Leave Blank)	2. REPORT DATE	3. REPORT TYPE AND DATES COVERED
	9/08	Final - 10/24/06-10/23/07

4. TITLE AND SUBTITLE
Study of Wide Field of View Optical System Based on Animal Eyes

5. FUNDING NUMBERS
W911NF-07-1-0001

6. AUTHOR(S)
Duncan Moore

7. PERFORMING ORGANIZATION NAME(S) AND ADDRESS(ES)
University of Rochester, Institute of Optics, 409 Goergen Hall, Box, 270186, Rochester, NY 14627-0360

8. PERFORMING ORGANIZATION REPORT NUMBER

9. SPONSORING / MONITORING AGENCY NAME(S) AND ADDRESS(ES)
U. S. Army Research Office
P.O. Box 12211
Research Triangle Park, NC 27709-2211

10. SPONSORING / MONITORING AGENCY REPORT NUMBER
W911NF-07-1-0001

11. SUPPLEMENTARY NOTES
The views, opinions and/or findings contained in this report are those of the author(s) and should not be construed as an official Department of the Army position, policy or decision, unless so designated by other documentation.

12 a. DISTRIBUTION / AVAILABILITY STATEMENT
Approved for public release; distribution unlimited.

12 b. DISTRIBUTION CODE

13. ABSTRACT (Maximum 200 words)

This study examines the compound eye and its potential role as a wide field of view optical system. A prototype system based on the apposition compound eye is designed and built. An alternate design based and the neural superposition compound eye is also presented. The effects of incorporating gradient index lenses into the system are also examined, as well as potential manufacturing methods.

14. SUBJECT TERMS
Insect vision, wide field optical systems, compound arrays

15. NUMBER OF PAGES
37

16. PRICE CODE

17. SECURITY CLASSIFICATION OR REPORT	18. SECURITY CLASSIFICATION ON THIS PAGE	19. SECURITY CLASSIFICATION OF ABSTRACT	20. LIMITATION OF ABSTRACT
UNCLASSIFIED	**UNCLASSIFIED**	**UNCLASSIFIED**	**UL**

NSN 7540-01-280-5500

Standard Form 298 (Rev.2-89)
Prescribed by ANSI Std. 239-18
298-102

Enclosure 1

University of Rochester
Grant No. W911NF-07-1-0001
Final Progress Report

Study of wide field of view optical systems based on animal eyes

PI: Duncan T. Moore

Abstract

This study examines the compound eye and its potential role as a wide field of view optical system. A prototype system based on the apposition compound eye is designed and built. An alternate design based and the neural superposition compound eye is also presented. The effects of incorporating gradient index lenses into the system are also examined, as well as potential manufacturing methods.

Introduction

Almost every animal on the planet that has a vision system can be classified as having a simple eye, or a compound eye. Simple eyes, sometimes called camera eyes, like our own human eye, can achieve high resolutions and a field of view of slightly higher than 180 degrees. The simple eye configuration that uses a single optical system to form an image on a detection plane is the standard used in the vast majority of vision and imaging technology. Compound eyes, found on almost all insects and crustaceans, have not yet had an artificial counterpart find its way into our technology. The closest comparison that is widely used today would be the gradient index rod arrays used in

scanners. Now the functionality of the scanner is not directly reflected in nature's compound eye, however the space and weight advantages are clearly apparent. The following sections cover the basic eye type, a unique compound eye type, and then briefly discuss when the compound eye is an advantageous choice.

Vision systems in nature

Over the course of time nature has evolved many distinct visual systems, and evidence suggests many of these systems developed independent of each other [**1,2**]. As it turns out, many of the evolutionary roads have lead to the same place. Although the fine details may expose fundamental differences, functionally, there are only a few different varieties of eyes. The two major eye types are the camera (or simple) eye and the compound eye.

The earliest known vision systems in nature are compound eyes. They have been identified on fossilized trilobites dated over half a billion years old. Compound eyes have anywhere from a few to tens of thousands of narrow light collecting cells groups called ommatidium. Each ommatidia is an individual optical system that typically includes a corneal lens, crystalline cone, and rhabdom (the equivalent of a simple eye's photoreceptor) [Figure 1]. These ommatidium are packed together into a hemispherical or cylindrical shape to form an eye with a nearly uninterrupted field of view.

There are two types of compound eyes, superposition eyes, and apposition eyes. In superposition eyes, an erect image is formed on the retina by superimposing light from multiple lenses [Figure 2]. Two important factors make this possible. The first is a long

clear zone between the optics and the rhabdom. In this region cells lack any absorbing pigment, allowing light to pass into adjacent ommatidia. The second is the unique gradient index property of the crystalline cones. Each one is nearly afocal, similar to a telescope. Research on artificial superposition systems has been previously demonstrated [**3**]. The general concept of this imaging has been utilized for years in copiers and scanners that use an array of gradient index rods.

In apposition eyes, each ommatidia is optically independent from its neighbors. Each lens system images onto the distal tip of its respective rhabdom [Figure 3]. An individual ommatidia does not gather any spatial information, it is effectively just a photocell. The spatial resolution is determined by the acceptance angle of the ommatidia and the angle between ommatidial axes. Typically, the acceptance angle is approximately equal to the angle between ommatidial axes, thus the field of one rhabdom 'apposes' its neighbors. Crystalline cones in some apposition eyes have strong gradient index properties. These are typical in aquatic and amphibious creatures that have little to no power in the corneal lens. Butterflies have apposition eyes with gradient index cones that work similar to those found in superposition eyes. The afocal gradient index cones make the system up to 10% more efficient for on axis light collection [**4**]. Rhabdom in apposition eyes are relatively long, a few hundred micrometers, and only 1-2 micrometers wide. Their refractive index is higher than the surrounding medium causing it to behave as a light guide, channeling light through the photoreceptive medium (microvilli).

As opposed to the compound eye, the other major type of imaging lens systems evolved for animal vision is the camera eye. Camera eyes are widely adopted by different

species including fish, birds, reptiles and mammals. A camera eye usually has a larger aperture size to achieve higher image resolution, and a few lenses to provide the optical power. In some species, their camera eyes have developed the zoom capability to image objects at different distances, a process commonly referred to as accommodation. This zoom process is usually accomplished by a single element inside the eye chamber.

To give an example of the human eye, the crystalline lens behind the cornea serves as the zoom lens. The crystalline lens is an elastic material that is held in place inside the eye by the zonule fibers attached to the ciliary body. Its major function is to adjust the focal length of the human eye by changing its own shape during accommodation. Usually when the object is at infinity or for the far vision, the human eye has about 60 diopters of power; and when it accommodates it can acquire more than 70 diopters of power for a young eye (object as close as 10cm). The crystalline lens is also a GRIN lens because the lens body is filled with fully compact lens fibers with different values of refractive index. It has core index of 1.406 and cortex index of 1.386. The index gradient is built up both radially and axially, and the isoindicial surfaces take on an ellipsoidal shape, which can provide the eye with higher optical power than a homogeneous lens. When the human eye accommodates, the crystalline lens rounds up and takes on a more spherical shape. Four major changes occur during this process. First, the curvature of the lens increase; second, the thickness of the lens increases; third, because the lens bulges out towards the cornea therefore the depth of anterior chamber decreases, and last but not least is the change in the of isoindicial surfaces of the GRIN profile. By our own experience, we know the image quality of our eyes is well maintained during accommodation, which

means the crystalline lens, as a single zoom element, not only provides extra power for near vision , but also keeps the aberration value down to preserve the image resolution throughout the focusing range. The ability of the crystalline lens by itself to maintain the image quality is the combinational effect of the change in the lens shape and the change in its GRIN profile. Undergoing research is trying to mimic the zoom effect of the crystalline lens by using flexible materials, for instance a liquid lens. However, without the incorporation of the GRIN in the lens, it is almost impossible to achieve the optical performance demonstrated by the human crystalline lens.

Neural Superposition Eye

Two-winged flies, and a handful of other insects, belong in a special subcategory of apposition eyes. These eyes have an array of rhabdomere located in the same ommatidia [Figure 4b]. It was first thought that they may have limited ability to resolve images, but the correct reason was identified in 1967 by Kuno Kirschfeld [**5**]. In these eyes, the angle between the fields of view of adjacent rhabdom (in the same ommatidia) is the same as the inter-ommatidial angle. Also, the rhabdomere in a single ommatidia are arranged in an analogous pattern to the ommatidium array. This suggests that seven rhabdomere in seven different ommatidia are looking in the same direction with overlapping fields of view [Figure 4 a,c]. Below the optical layers a neural network links the signals from the seven rhabdomer to the same lamina (a nerve center located between the rhabdom and brain). As far as the brain is concerned, the signal appears the same as a

normal apposition eye, except the photon capture is seven times greater without sacrificing spatial resolution. Kirschfeld called this system 'neural superposition.'

This unique arrangement is one of the models for the artificial system observed in this study. No research has been done on developing the optical design based off of the neural superposition eye. There are several advantages to this design. Photon capture will be greater than in a standard apposition arrangement. Signals from networked detectors in different ommatidia can be averaged to improve the signal to noise ratio. The superposition of signals can be used to gather more sensitive time derivations. Furthermore, this arrangement allows for a unique transmitter/detector arrangement. For example the central element on the array would be a transmitter, like a VCSEL, and off axis elements would be detectors. Fiber optics can be used to carry the information from the image plan of the lens array to an arrangement of transmitter and detector arrays [Figure 5]. With this arrangement you can transmit and detect in the full field of view, and furthermore, with multiple detectors sharing the same acceptance angle, some detectors could gather information like color and polarization.

Advantages of compound eyes

The applications and advantages of simple eyes are very well know, so here we will focus on compound eyes and why nature has found them to be the optimal micro vision system.

An obvious advantage of the compound eye is its enormous field of view. Some can see in almost every direction without having to move a muscle. But this wide field

advantage is severely restricted by a relationship between spatial resolution and eye size. In the simple eye, the radius of the eye increases linearly with resolution, but for compound eyes, it increases by the square of the resolution. Details are discussed in the next section and additional information can be found in references [**5-7**]. This limiting physical relationship is why there are no large compound eyes found in nature, or with relatively high resolution. As body size increases and more resolution is necessary, nature has adapted to move the eyes and/or head to look around, as well as support larger brains for more complex visual processing. Compound eye optics are also less complex from a design standpoint. Compound eyes operate on non-imaging principals and do not suffer significantly from aberrations. They also have depth of field extending from a few millimeters to infinity as a result of having a short focal length. Simple eyes require a moving or deformable optic (like the human crystalline lens) to refocus or zoom to achieve imaging for objects at various distances.

Looking back at small visual systems, the diffraction limit and photoreceptor size become constraining factors. The small vision systems are where compound eyes have the advantage. Resolution for both systems is still comparable; however, compound eye's wraparound architecture is more compact, lightweight, and can have an extremely wide field of view. A simple eye has the disadvantage now of having a limited field of view per eye, the need to keep the eye internal for protection, and any added mechanisms for eye movement control. Simple eyes have a clear internal volume so the light can pass through from the optics to form an image on the photoreceptors. This volume takes up

space and adds weight making the compound system a more optimal choice for smaller systems.

How visual information is processed in compound eyes versus simple eyes is significantly different, and plays an important role in the biology of the nervous system and the optics. Typically the more resolution you have the more processing power required, more megapixels more data to sift through. Compound eyes operate on slightly different principles to extract valuable information with limited resolution. Their vision system and neural responses are streamlined to respond to what is essential for survival. Compound vision involves parallel processing techniques that are not widely used in standard imaging technology today. Optical flow and hyperacuity [**8**] are examples of these techniques. The details of how processing is accomplished in animals is not the focus of this study, however, the required optical response is important and techniques on how to tailor the optical design to achieve a desired response are discussed later.

These comparisons provide a basis for when an artificial compound eye is an appropriate optical solution. Like in nature, its primary application is in micro vision systems for robotics and unmanned micro vehicles. Such systems can accomplish object identification, motion detection, distance verification, object avoidance, and can even be adapted to provide color images, IR vison, polarization information, and send and receive optical communications.

Artificial Compound Eye Design

A geometrical model of an artificial compound eye [Fig 6,7] is sufficient to understand the basic design form and why there is a profound limitation to a compound eyes spatial resolution. An average insect has a spatial resolution around 1 cycle per degree, very poor compared to a humans 60 cycles per degree. In order to improve the resolution the size of the eye must increase, but this is where compound eyes eventually become impractical.

The radius of a compound eye is:

$$R \approx 2Dv_s \quad \text{or,} \quad R \approx D/\phi \ , \ \left(v_s = 1/(2\phi)\right) \tag{1}$$

where R is the radius, ϕ is the inter-ommatidial angle, D is the pupil lens diameter of each ommatidia, and v_s the sampling frequency. For a diffraction limited system the acceptance angle is roughly $\Delta\rho \cup \lambda/D$, and the acceptance angle should match the inter-ommatidial angle ($\phi = \Delta\rho$). Then D can be substituted into equation one, yielding the relation:

$$R \approx 4\lambda v_s^{\,2} \tag{2}$$

For camera eyes [Fig. 8], the relationship between eye radius and sampling frequency is:

$$R \approx (f/\#)\lambda v_s \tag{3}$$

The size of a compound eye increases as the square of the spatial resolution. This is the likely explanation as to why all large eyes are camera type eyes, but also leads to an interesting point made by Wehner [**9**], "a bee scanning objects parallel to the horizon

exhibits an angular resolution 160 times poorer than man. A bee can resolve the same number of points as we do by just viewing the object from a distance 160 times smaller."

The geometry of an apposition or neural superposition compound eye does not have many degrees of freedom [Fig 7]. If the overall size (R) and resolution (ϕ) are chosen, the two most important factors for making a practical device, then only one more variable can be chosen as they are all directly related, focal length (f), lens radius (r), numerical aperture, and image size (s). In a system that incorporated a transmission source, the specifications are driven by the numerical apertures of the system and the transmitting source.

With these constraints a first order model is easily generated. An excel spread sheet provides a fast analysis on how to set up a system for a desired size and resolution. See Table 1 for an example of a first order analysis. The next step is to examine the angular response of coupling light to the photo receptor [Fig. 9]. This response directly effects how the visual information is processed. There is an abundance of research on the angular responses of apposition compound eyes for natural and artificial systems [**10-13**]. Natural systems are near diffraction limited and are similar in response to coupling light into single mode fiber. They typically have Gaussian angular responses [**13**], with varying amounts of crossover between ommatidia **[14]**.

The Excel table was expanded to generate a more complete geometrical model for either apposition or neural superposition systems [Table 2]. Data from the table are then transferred to LightTools, an optical modeling software package from Optical Research Associates, to generate a detailed optical analysis and make any modifications

for performance requirements. Various modifications of the geometrical model can be used to tailor a desired response performance. It may need to match a natural system or be for a unique optical or signal processing solution. By changing physical properties of focal length, lens curvature, detector size and position, an artificial system is easily customizable. Additional methods include specifying aberrations in the optic(s), using a gradient index media, or adding secondary optics. These are all properties and techniques that can adjust the acceptance angle of the photoreceptors, the inter ommatidial angle (ϕ) that governs the overlap or crosstalk between neighboring receptors, and the specific response figure (Gaussian, top hat, triangular, see Fig. 10). Figure 11 is a system generated in LightTools that is designed to produce a response similar to the house fly *Musca domestic* **[13]**. Figure 12 shows the Gaussian response of neighboring photoreceptors with ~75% overlap as a source is scanned across the field.

The following section shows an example of how the system responds to changes in its physical geometery. This helps explain how to customize the system for a desired signal response as well as providing a set of tolerances for design sensitivity. Figure 13 shows a seven ommatidia mockup generated in LightTools to carry out the following tests. First, the lens radius (r) of the system was varied to study the effects of defocusing on the photoreceptors of a fixed position. In this model the photoreceptors are simulated as fiber optics. Figure 14 shows the photoreceptor response to scanning a 1mm circular source across the visual field, at both 20cm from the system and at infinity for several different values of r. With the lens radius held constant, the position of the photoreceptors (f) was also varied to study the photoreceptors angular response. Figure

15 shows the behavior of the system to a 1mm circular source scanned across the visual field at both 20cm from the system and at infinity for several different values of f. Take note that in the case of an apposition system changing the position of the photoreceptors will result only in changing the overlap of neighboring responses and their photoreceptor response profile, but in a neural superposition system it will also misalign photoreceptors that shared the same filed of view, however, some misalignment may be beneficial to the signal processing [14].

Tapered Gradients

Gradient index lenses can be found in both compound eyes and camera eyes. Incorporating a gradient index into an artificial system provides an additional degree of freedom that can be used to fine tune focal length, image size, and numerical aperture. For an artificial system it is advantageous to use a gradient index to shorten the focal length, leaving as much room as possible for hardware that needs to fit inside the enclosure of the lens array.

Equation 4 represents the gradient index profile of a simple radial gradient.

$$N(r) = N_0 + N_1 r^2 + N_2 r^4 + \ldots; (4)$$

This equation can be used to derive the paraxial formulas of ray behavior in the gradient index medium. Here is the profile representation of a linear tapered gradient:

$$N(r,z) = N_0 - N_1 \frac{r^2}{(1 - za/y_m)^2}; (5)$$

See Figure 16a: N_0 is the base index along the central axis, N_1 is a constant, a is the taper angle, y_m defines the edge of the taper at z=0, y_0 is the starting ray height, u_0 is the starting ray angle. The linear model will be used here for an example of meridional ray tracing (y,z) inside a tapered gradient index. Applying this profile to the ray equation [**15**],

$$\frac{\partial N}{\partial z}(1+\dot{y}^2)\dot{y} + N(y,z)\ddot{y} - (1+\dot{y}^2)\frac{\partial N}{\partial y} = 0;(6)$$

one can derive the paraxial equations for rays traveling through a linear tapered medium[**16**]:

$$Y(z) = y_0\sqrt{\tilde{z}}Cos[b*Log[\tilde{z}]] - \left(\frac{u_0 y_m + y_0 a/2}{ab}\right)\sqrt{\tilde{z}}Sin[b*Log[\tilde{z}]];(7)$$

$$\tilde{z} = (1 - za/y_m);b = \sqrt{\frac{2\Delta n}{N_0 a^2} - 1/4}$$

Figure 16b shows the behavior of paraxial rays in a tapered gradient (dark or black ray) compared to a typical radial gradient (green or gray ray). The rays in the tapered gradient continue to experience angular magnification as they traverse towards the end of the taper and eventually escape out the side, or possibly bend around and continue back out of the taper. The tapered gradient has a shorter focal length and higher numerical aperture that is dependent on the angle of taper (a). This relationship between taper angle and the distance to the back focal point is derived from equation 7. Distance to back focal point z as a function of taper angle a:

$$z(a) = \frac{y_m}{-a}\left(e^{\left(\frac{ArcTan(2b)-\pi}{b}\right)} - 1\right);(8)$$

Figure 17 shows the almost linear relationship between the taper angle and the focal length.

The next step will be to expand the solution into terms that can be used to determine third order aberrations. The linear taper may not be a suitable model for the actual tapered lenses. It will likely be based on a diffusion model that is similar to concentric cones or concentric radial symmetric hyperbolas. Also, since the oscillating rays in tapered gradients are continually experiencing magnification, it will be important to know the accuracy of a paraxial model. Several models have been encoded into CodeV in order to numerically trace the real rays [Fig. 18].

There is currently no published work that discusses chromatics in tapered gradient index lenses. Preliminary results, observing the linear taper case, suggest that in some cases the taper has a significant effect on chromatic behavior that is worth future investigation.

Artificial Apposition System

An artificial apposition compound array prototype was built for DARPATECH 2007. The motivation was to provide an alternative optical design for a low resolution camera style optical system used for tracking a moving target. Figure 19 is the nineteen element prototype designed in LightTools. From this design seven and nineteen element prototypes were built (Fig. 20 and 21). They have an inter ommatidial angle of 5

degrees, system field of view is 25 degrees, and the system radius of curvature is 60mm. Light is coupled into large core plastic optical fibers to provide a flexible method of connecting the system to detectors or transmitters. Details of the prototype's physical layout are in Table 3.

The optical material for the lenses is a silicone elastomer from NuSil, R-2615 (index of refraction n = 1.41). It is a two part thermal setting elastomer. The fibers come from Edmund Optics (J02-534). The cladding is 1mm diameter with index 1.402, the core diameter is 980um with index 1.492. The one millimeter diameter fibers where chosen to keep alignment tolerances in the limits of the holder manufacturing process. Fibers with a smaller diameter can be used if a shorter system length is required and they will also have a smaller bending radius. The frame and holder are made by Design Prototyping Technologies (DPT) using stereolithography (SLA).

To make the lens array first a pattern mask is printed onto a transparency using a laser jet printer. The appropriate volume on UV curable resin (Norland 61) is dispensed onto the mask at all nineteen positions forming the correct spherical radius needed. After curing the droplets onto the mask, the thermal setting silicone elastomer is poured over the mask and droplets to form the negative mold for the outer surface of the compound lens array. The mold for the inner side of the array was made by DPT's stereo-lithography process. The two molds are spaced apart by plastic shim stock (250um) and filled with the optical silicone elastomer. Fibers are inserted into the back of the DPT mold to form the positions that they will later be permanently fixed at. Once the silicone compound array is thermally set it is placed into the frame and holder that will keep each

lenslet in the proper position. Figures 22 and 23 show the pieces of the mold, the frame, and the pattern mask. Finally the fibers are inserted into each lenslet and fixed there with additional silicone. For the seven element system, each lenslet was made individually and is not permanently fixed into the holder. Figure 24 shows the angular response of three adjacent lenslets in the final artificial apposition array. This data matches the specification from Table 3. The dip in the peak of the left response curve may be due to a micro air bubble that was trapped in the mold. It was difficult to remove air bubbles from the steep cone shapes even using a low vacuum. Also, the central response curve has a steep left side. This may also be due to an air bubble, or accidentally stripping off the thin cladding on the 1mm fiber.

Artificial Neural Superposition System Design

The apposition system built in the previous section was designed with the potential to be modified into a neural superposition system. This section will present the neural superposition design and variations for converting the artificial apposition system.

Figure 25 is a nineteen element LightTools neural superposition model. Each ommatidia supports seven fibers, requiring a total of 133. Geometrical details of the ommatidia and fibers are provided in Table 4. This was the original design for the neural apposition system. It has equal resolution to the artificial apposition system, and the overall field for a nineteen element system is 35 degrees plus another +/-5 degrees of under sampled region from the off axis fibers in the outer ring of ommatidia. The

solution in Table 4 uses seven 250um diameter fibers located at a shorter focal length. The shorter focal length also results in a smaller corneal lens with stronger curvature. A larger fiber bundle solutions exists, but if it is too large the available volume is exceeded and the system can not be arrayed. For example the solution for using a bundle of seven 1mm diameter fibers is impractical because the diameter of the fiber bundle will exceed the diameter of the ommatidia at the focal position (assuming the ommatidium is no wider than its corneal lens diameter).

Conclusion

This study focused on the design and fabrication of an apposition compound array and its practical use as a wide field of view optical system. Its advantages over camera type optical systems where discussed. Seven element and nineteen element prototypes were fabricated in the lab from commercially available materials and using basic model building techniques. The final prototypes matched the design specification and were shown at DARPATECH 2007.

A close derivative of the apposition system, the neural superposition compound array, found in fruit flies and other two winged flies, was also studied. It has several differences from the apposition system that make it an attractive candidate for an artificial vision system. Its unique design and potential advantages were presented in detail. A prototype was designed and can be made with only minimal modification to the fabrication process of the apposition prototype. The work in this study can help other programs, like the machine vision program at University of Wyoming [13], design and

build systems to further research in the fields of machine vision and bio inspired optical systems.

Gradient index optics, found in a great many vision systems in nature, are also discussed as they provide several system advantages which nature has already capitalized on. Modeling work is presented that can be applied to future design and fabrication methods for compound array systems.

Biologically inspired wide field optical systems like the ones presented here have massive potential to improve upon the next generation technology.

References

[1] T.H. Goldsmith, "Optimization, constraint, and history in the evolution of eyes", Quarterly Review of Biology, Vol. 65, 281-322, 1990

[2] M.F. Land, R.D. Fernald, "The evolution of eyes". Annual Review of Neuroscience, vol 15, 1-29, 1992

[3] J. Robert Zinter, "A three Dimensional Superposition Array", Masters Thesis Institute of Optics, University of Rochester NY, 1987.

[4] D.E. Nilsson, M.F. Land, "Optics of the butterfly eye", J Comp Physiol A, Vol 162, pg 341 366, 1988

[5] K. Kirschfeld, "The Resolution of Lens and Compound Eyes", Neural Principles in Vision (Eds. F. Zettler, R. Weiler), pg 354-370, 1976

[6] M. Land, Facets of Vision (Eds. D.G. Stavenga, R.C. Hardie), "Variation in the structure and design of compound eyes", Chap 5, pp 90-111, 1989

[7] Jeffery S. Sanders, Carl E. Halford, "Design and analysis of apposition compound eye optical sensors", Optical Engineering, Vol. 34(1), pp 222-235, 1995 SPIE

[8] T. Poggio, M. Fahle, and S. Edelman, "Fast perceptual learning in visual hyperacuity" Science, Vol 256, Issue 5059, 1018-1021, © 1992 American Association for the Advancement of Science

[9] R. Wehner, "Comparative Physiology and Evolution of vision in Invertebrates", Vol. VI/C, Invertebrate Visual Centers and Behavior II, Spatioal Vision in Arthropods, Springer-Verlag, New York, 1981

[10] G. A. Horridge , "The Separation of Visual Axes in Apposition Compound Eyes", Philosophical Transactions of the Royal Society of London. Series B, Biological Sciences, Vol. 285, No. 1003 (Dec. 5, 1978), pp. 1-59

[11] Adrian Horridge, "The spatial resolutions of the apposition compound eye and its neuro-sensory feature detectors: observation versus theory", Journal of Insect Physiology Volume 51, Issue 3, March 2005, Pages 243-266

[12] A Brückner, J Duparré, A Bräuer, A Tünnermann , "Analytic modeling of the angular sensitivity function and modulation transfer function of ultrathin multichannel imaging systems", OPTICS LETTERS, Vol. 32, No. 12, June 15, 2007

[13] D T Riley, W M Harman, E Tomberlin, S F Barrett, M Wilcox, C H G Wright, "Musca Domestica Inspired Machine Vision with Hyperacuity", SPIE proceedings Smart sensor technology and measurement systems. Conference, San Diego CA, 2005, vol. 5758, pp. 304-320

[14] B Pick, "Specific Misalignments of Rhabdomere Visual Axes in the Nerural Superposition Eye of Dipteran Flies", Bilogical Cybernetics, 26, pg 215-224, 1977

[15] D.T. Moore, "Aberration Correction Using Index Gradients", Masters Thesis, The Institute of Optics, University of Rochester, New York 1970

[16] S.J.S. Brown, "Geometrical Optics of Tapered Gradient-Index Rods", Applied Optics, Vol 19 No. 7, April 1980

Figure 1 Ommatidia

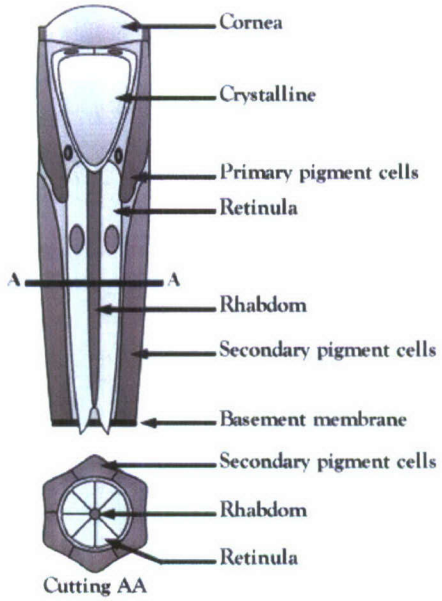

Figure 2 Superposition

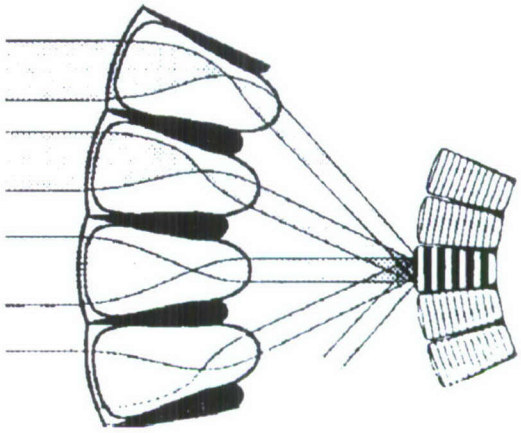

Figure 3 Apposition

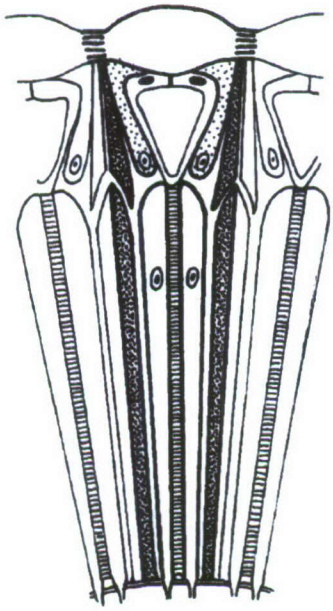

Figure 4 Neural Superposition

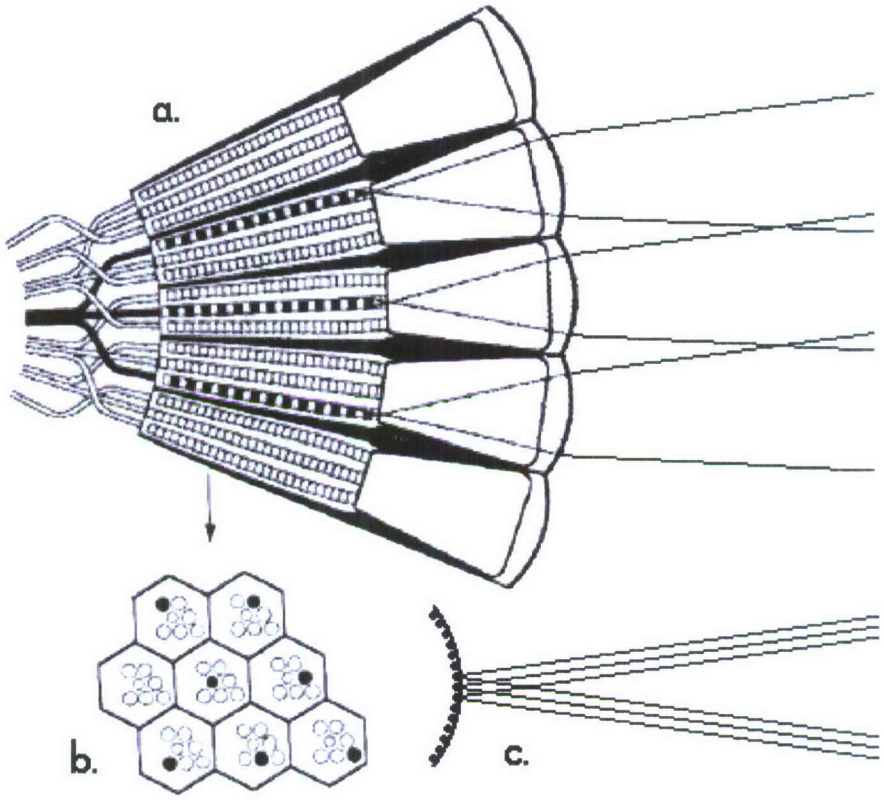

Figure 5

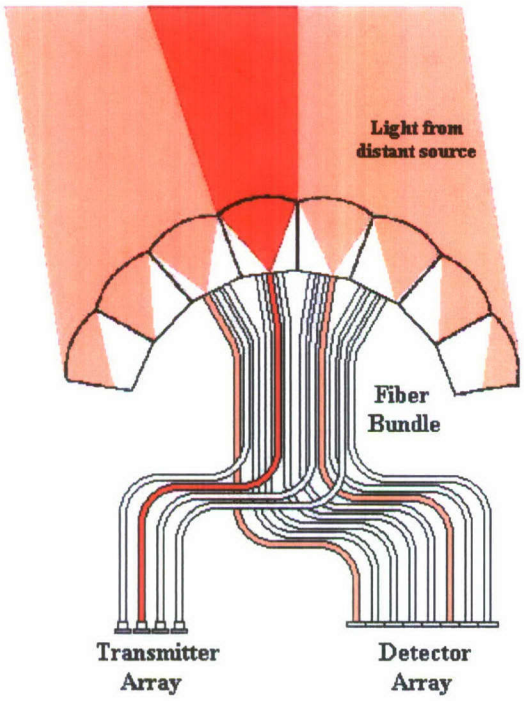

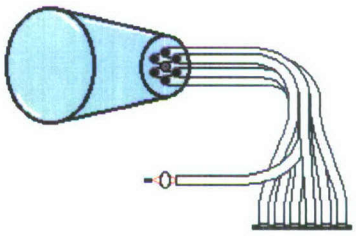

Single Lens Test Setup

Figure 6

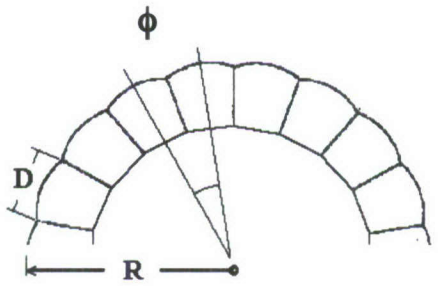

Figure 7

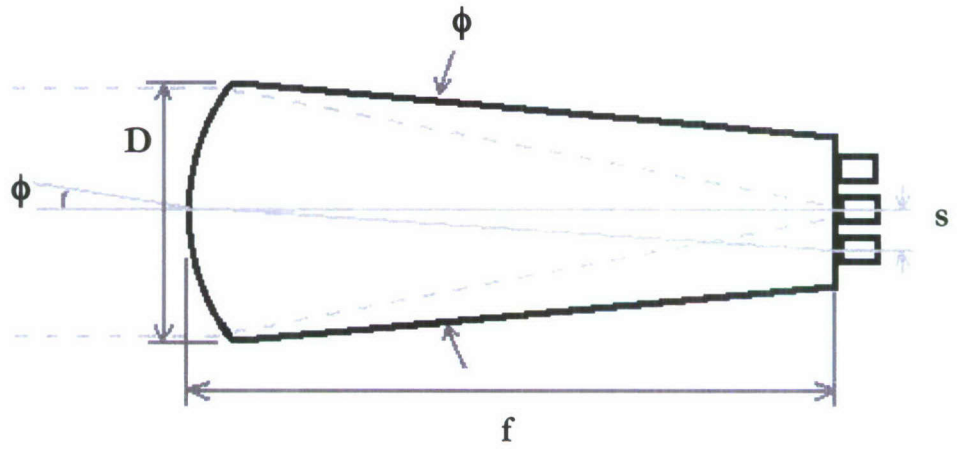

$$\phi \approx \frac{D}{R} \qquad f = n\frac{s}{\phi} \qquad r = \frac{f\,(n-1)}{n}$$

Figure 8

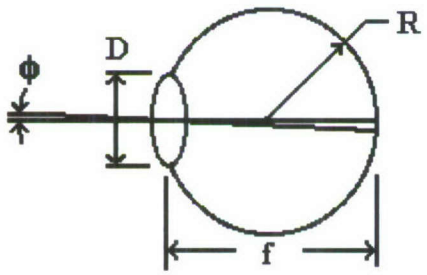

Figure 9 The acceptance angle ($\Delta\rho$)of an ommatidium results from a combination of the Airy diffraction pattern (point-spread function) given by **_/D** and the geometrical angular width of the rhabdom **d/f** as the nodal point of the lens. (Reference: Figure 7.6, p. 134, *Animal Eyes*, Michael F. Land, Dan-Eric Nilsson)

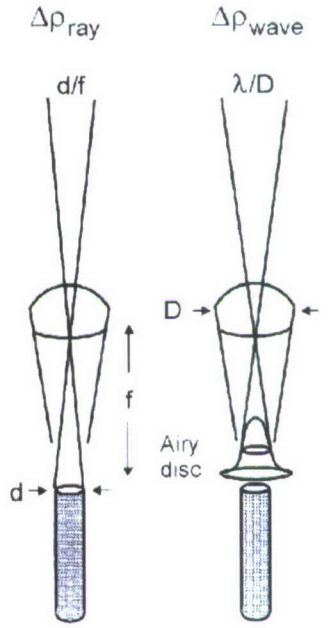

Figure 10

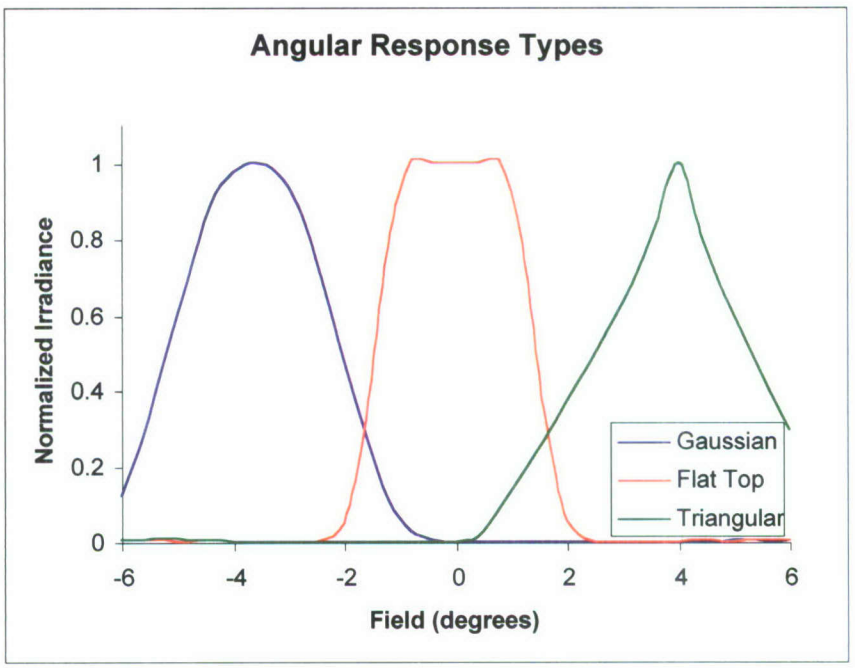

Figure 11

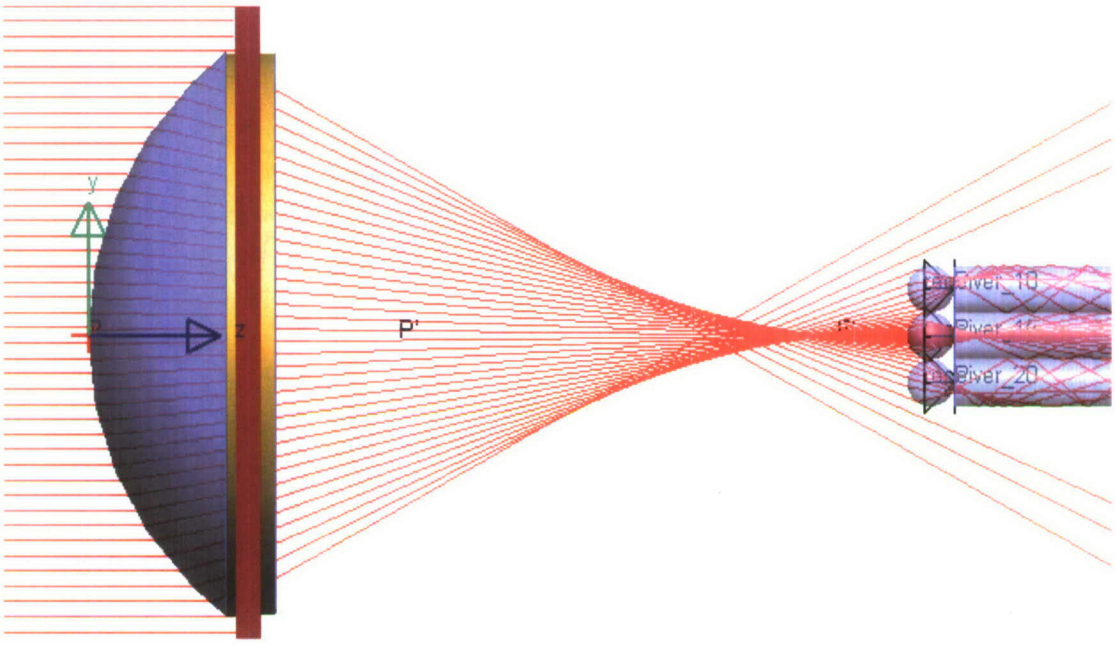

Figure 12

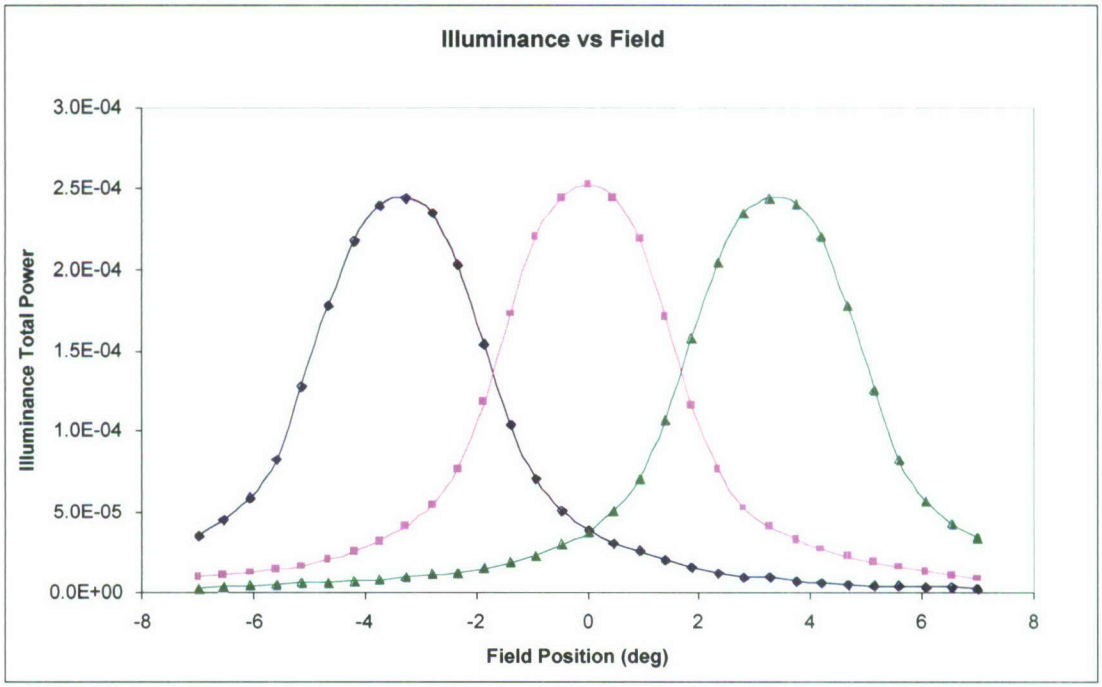

Figure 13

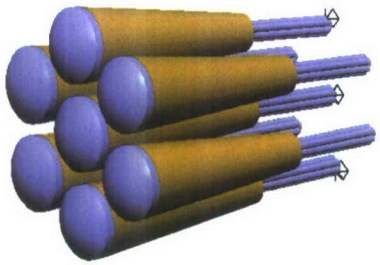

Figure 14 The angular response of radius of curvature changes from 1.96-2.46mm.

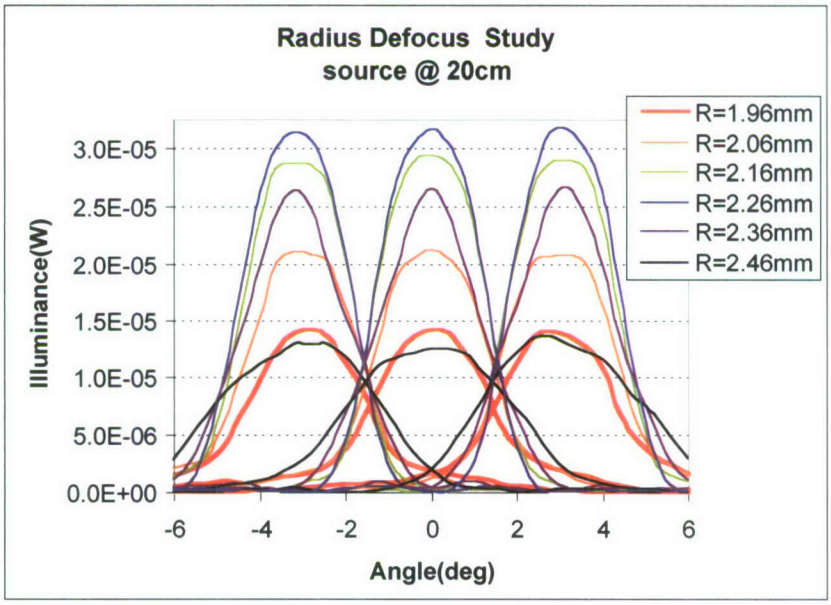

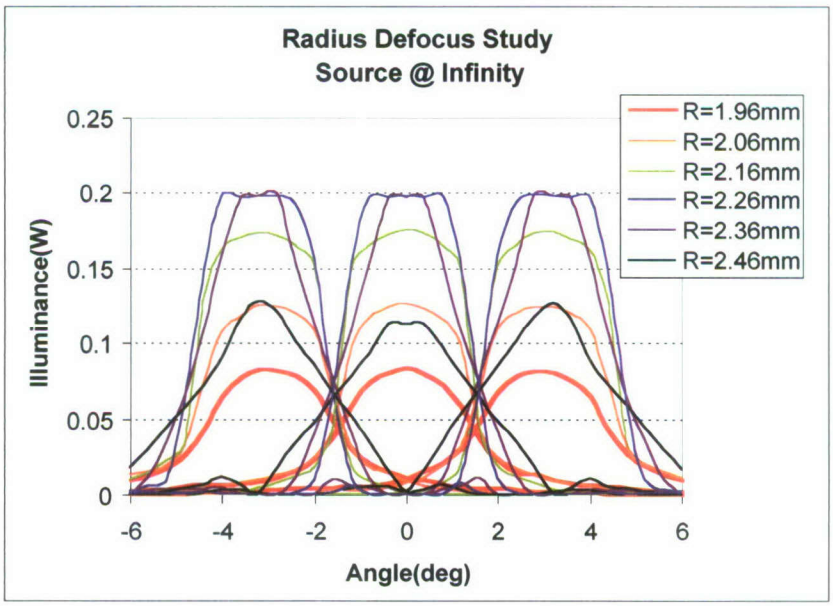

Figure 15 The angular response for focal length changes from 5.9-7.1 mm.

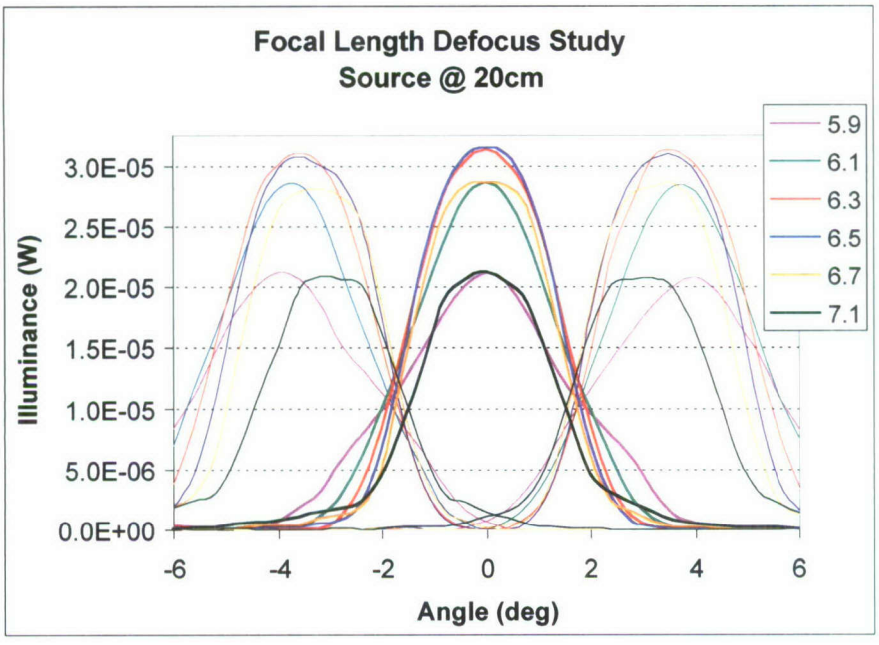

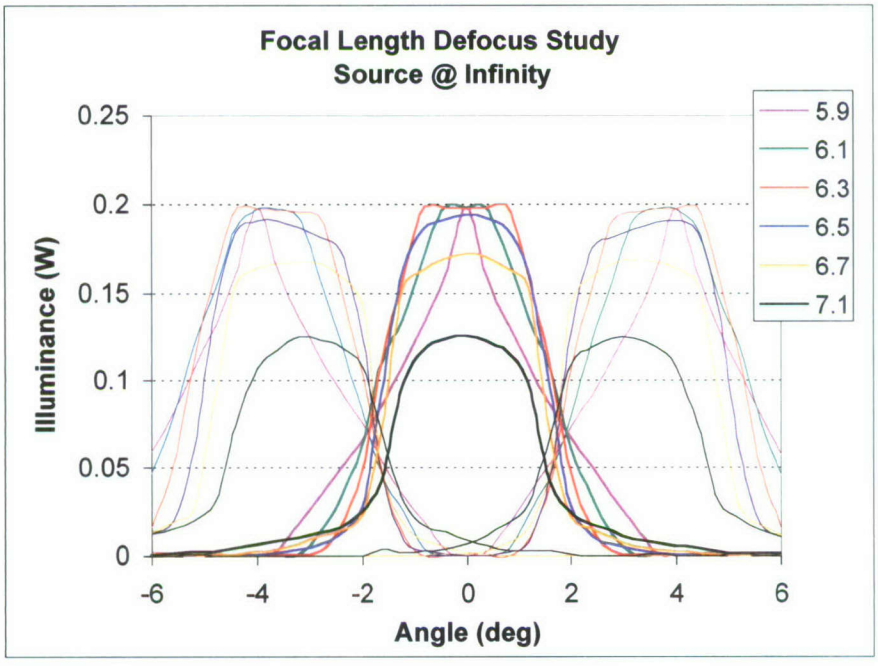

Figure 16a

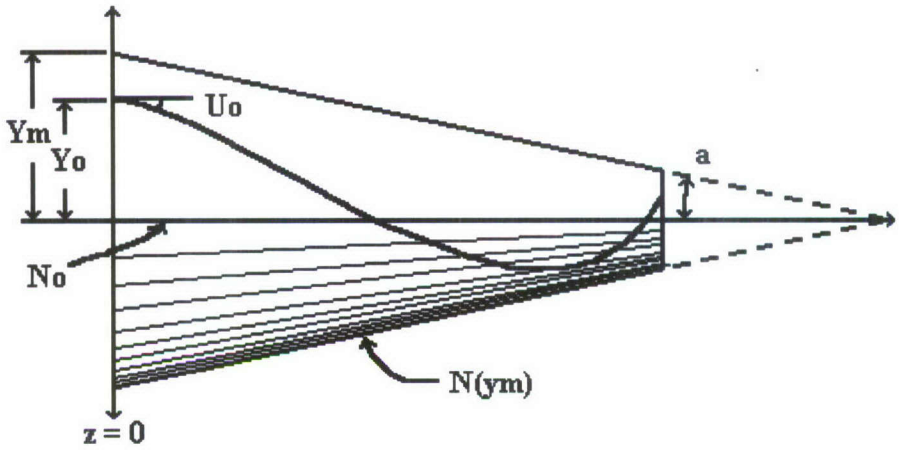

$$Y(z) = y_0\sqrt{\tilde{z}}Cos[b * Log[\tilde{z}]] - \left(\frac{u_0 y_m + y_0 a/2}{ab}\right)\sqrt{\tilde{z}}Sin[b * Log[\tilde{z}]]$$

$$\tilde{z} = (1 - za/y_m); b = \sqrt{\frac{2\Delta n}{N_0 a^2} - 1/4}$$

Figure 16b

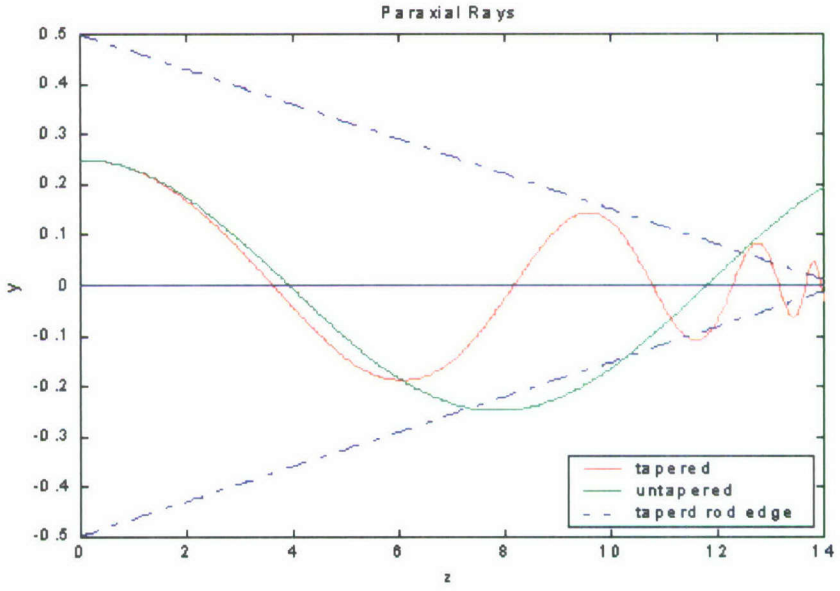

Figure 17

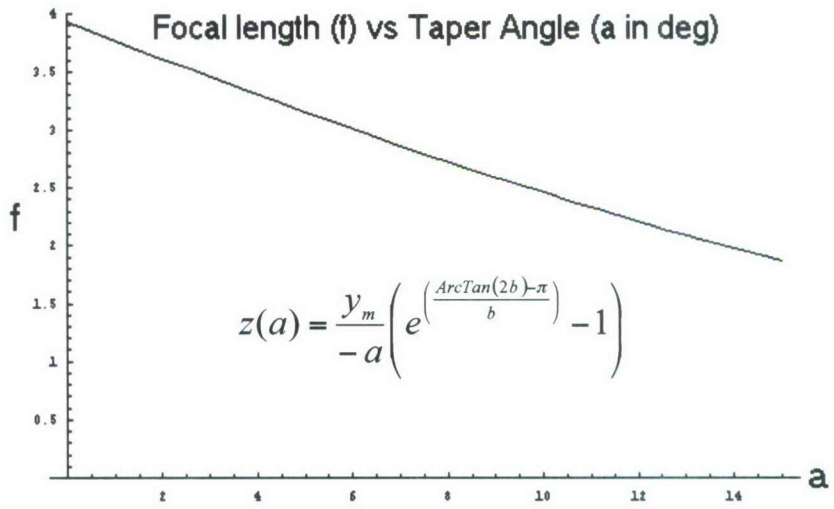

Figure 18

Weak Tapered Gradient Lens (a =1.25, dn =.1)

Figure 19

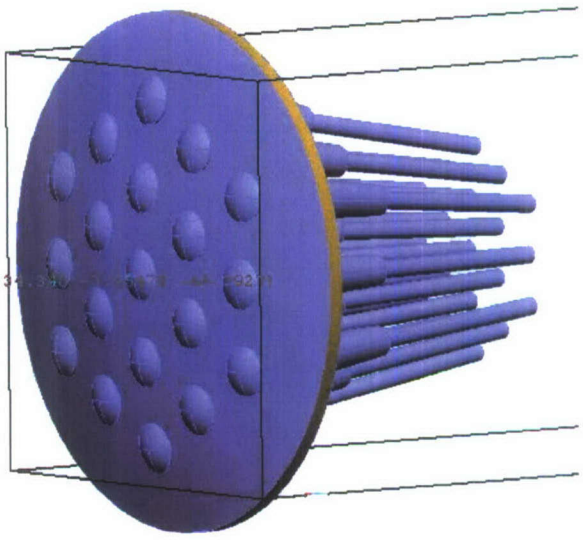

Figure 20 Seven and nineteen element apposition compound arrays with a single silicone ommatidium and fiber in the front.

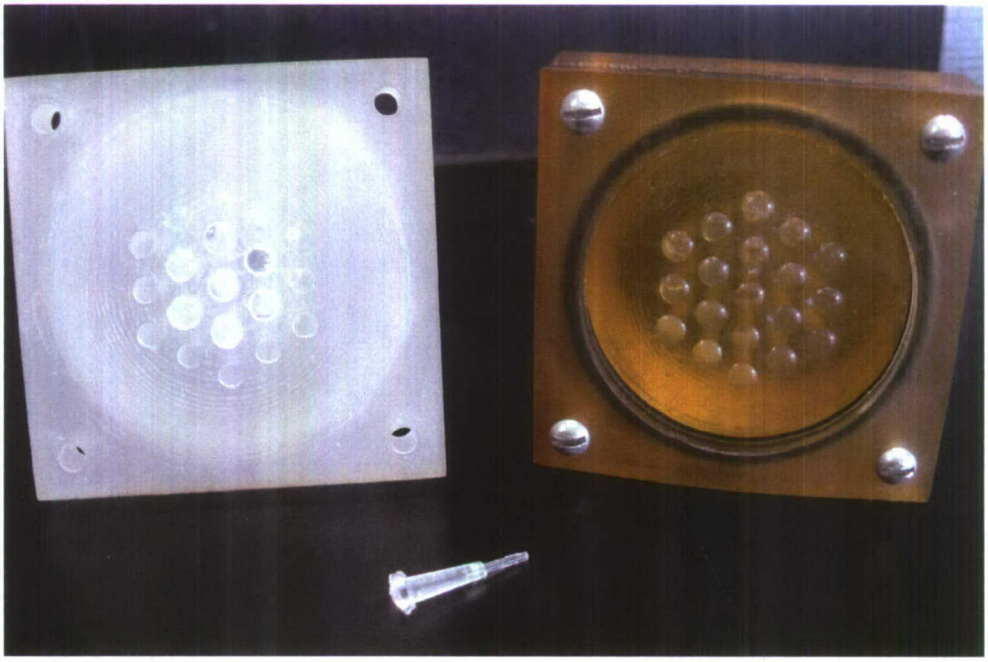

Figure 21 The seven element array with 1mm diameter fibers. The box in the lower right shows the fiber output. Seven fibers from the ommatia are bright, and the other fibers that are capped off are dark.

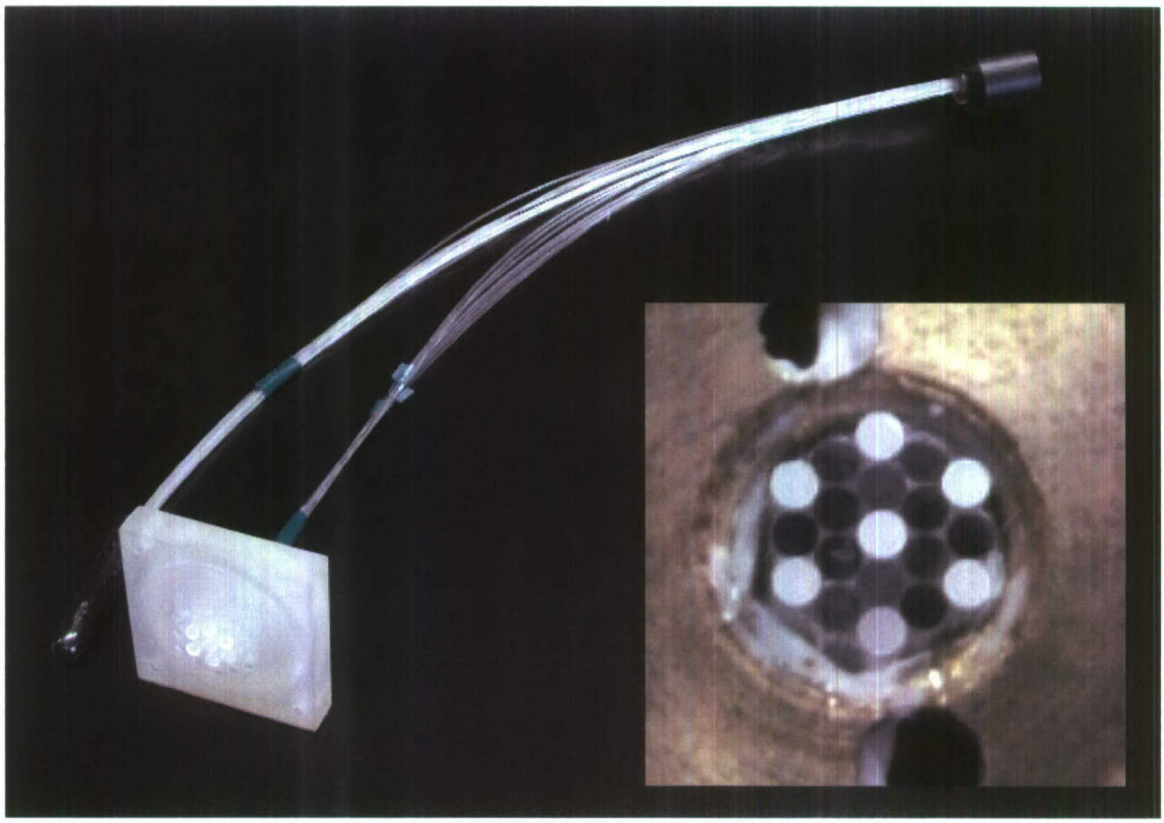

Figure 22 Caseing that holds the mold together while the silicone sets. The yellow block on the left is the back portion of the mold.

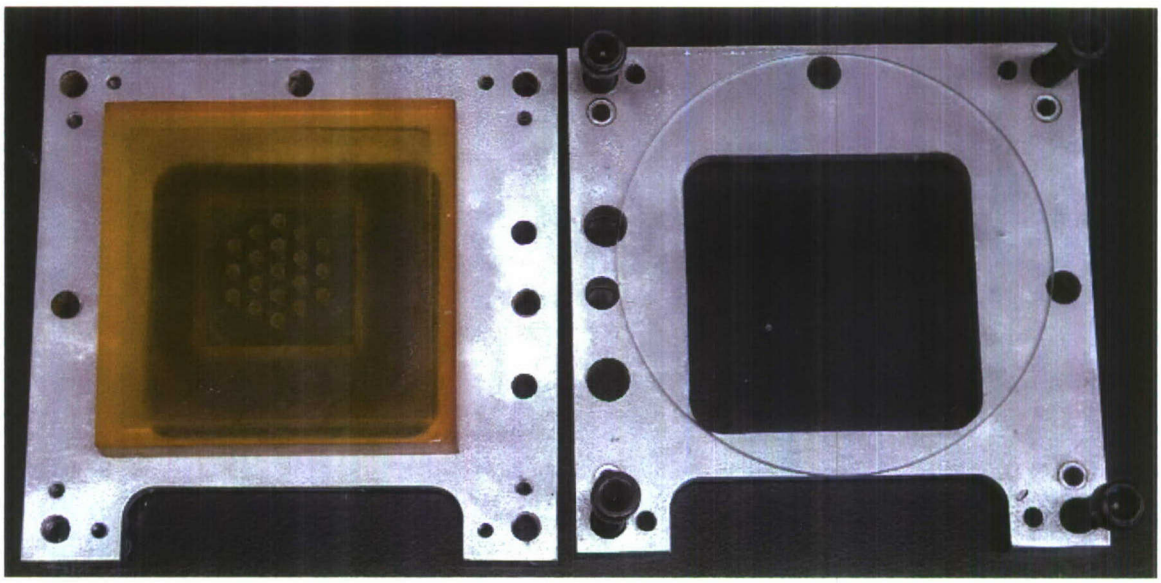

Figure 23

Top left, practice silicone lens array using the front mold and a flat glass back mold.
Top right, final negative mold used for the front of the compound apposition array.
Bottom left, mask with microlenses used for making the mold at top right.
Bottom right, a second mask with the 250micron shim stock

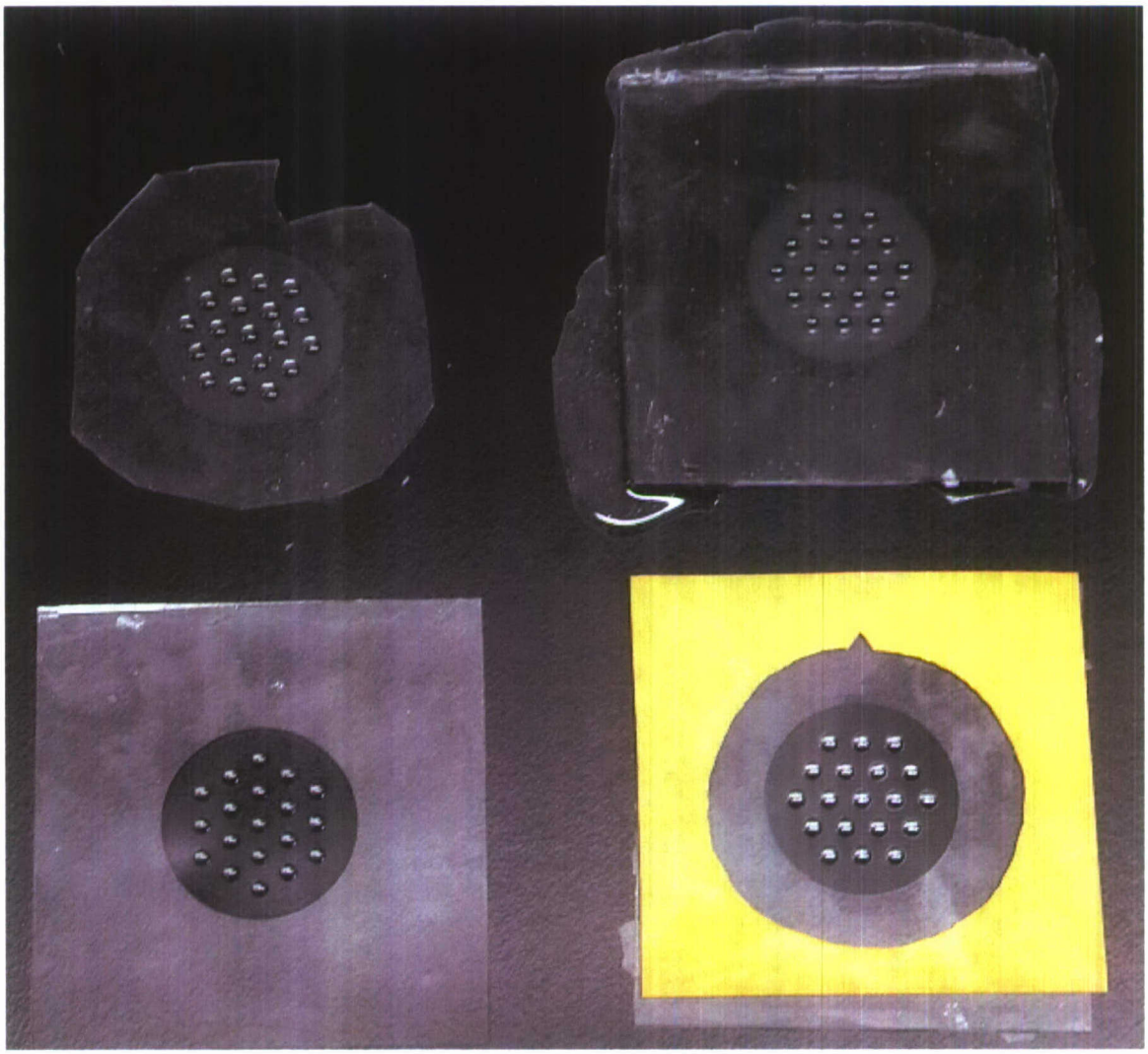

Figure 24

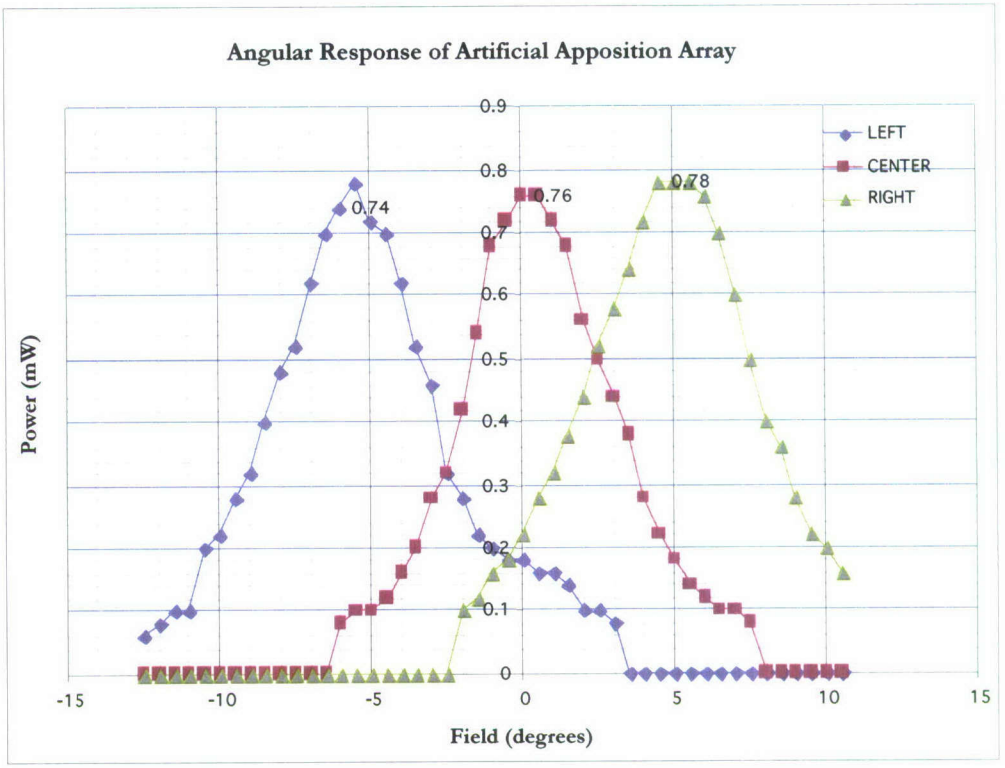

Figure 25

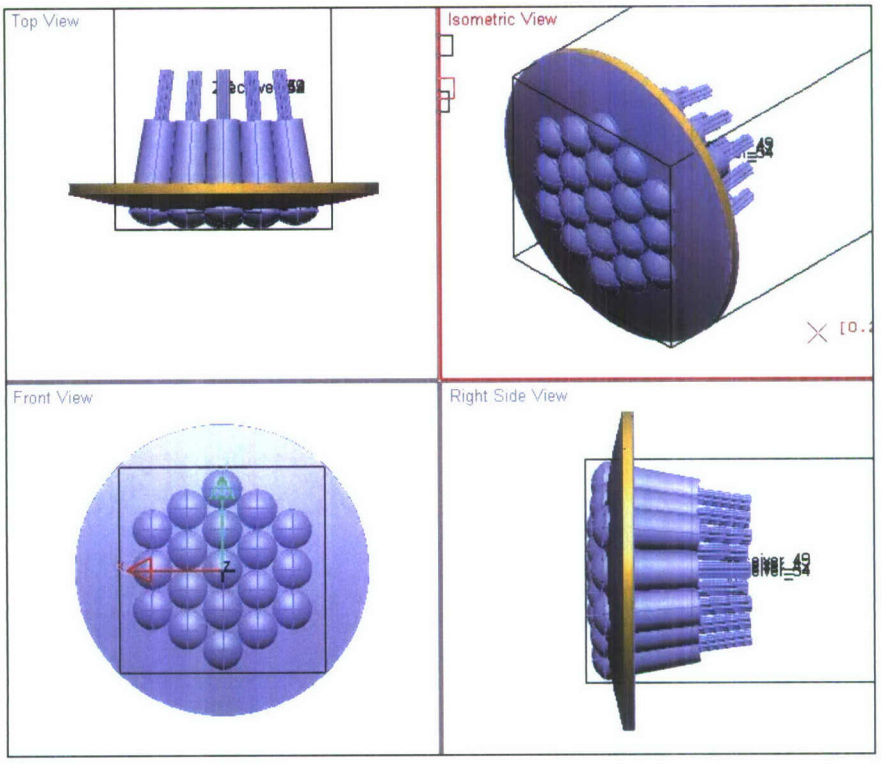

Table 1

Input		Output		Constraints	
Radius:	10				
Angular Resolution (deg):	3				
Index (n):	1.6				
wavelength	0.0005				
		Diameter:	0.523599		
				Max focal length:	3.478261
				Max Image height:	0.056913
				Max F/#:	6.642989
Ratio	0.016362	0.01713473			
Source Diamter:	0.04				
		focal length	1.22231		
		Source F/#:	2.33444		
Table in (mm)		**radius of curvature**	0.458366		
Paraxial Approx.		**half angle**	12.27185		
D(hex)= D(circular)*2/SQRT(3))					

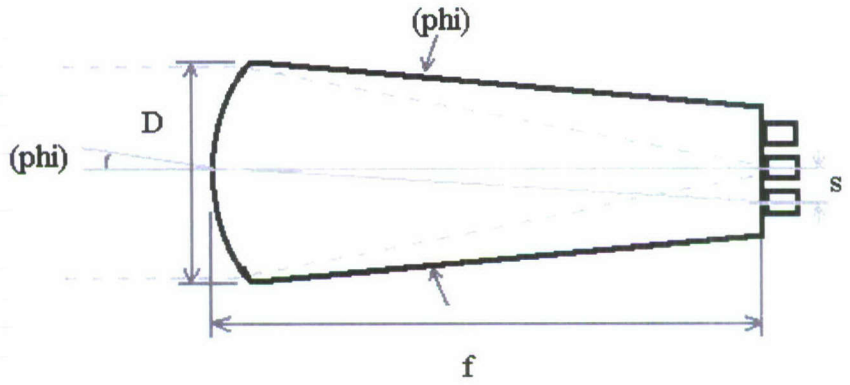

Table 2

Physical Properties	
System Radius (mm)	60
Lens Index	1.41
Lens Diameter (mm)	2.5
Lens Spacing (mm)	3.14
Lens curvature (radius mm)	2.06
Lens height (mm)	0.42
Distance to image plane (mm)	6.45
Central fiber core dia. (mm)	0.24
Cent. fiber clad dia	0.25
Off-Axis fiber core dia	0.24
Off-Axis fiber clad dia	0.25
Fiber NA (deg)	30.66
NA in lens (deg)	21.2

Design Specs	
Resolution	
Inter ommatidial angle (deg)	3
(overlap)	3.46
Central Field (deg)	3.00
Off-axis field (deg)	3.00
Hyperacuity	
Off-axis Field shift (deg)	0.13
Marginal focus (mm)	6.38
Full Fill B (bestfocus mm)	6.96
Paraxial focus (mm)	7.1

Table 3 Apposition Array Specifications

Physical Properties	
System Radius (mm)	60
Lens Index	1.41
Lens Diameter (mm)	3.5
Lens Spacing (mm)	5.23
Lens curvature (radius mm)	2.6
Lens height (mm)	0.67
Distance to image plane (mm)	10
Central fiber core dia. (mm)	0.98
Cent. fiber clad dia	1
Off-Axis fiber core dia	0
Off-Axis fiber clad dia	0
Fiber NA (deg)	30.66
NA in lens (deg)	21.2

Design Specs	
Resolution	
Inter ommatidial angle (deg)	5
(overlap)	5.77
Central Field (deg)	7.93
Off-axis field (deg)	0
Hyperacuity	
Off-axis Field shift (deg)	-0.95
Marginal focus (mm)	7.8
Full Fill B (bestfocus mm)	9.8
Paraxial focus (mm)	8.94

Table 4 Neural Superposition Array Specifications

Physical Properties	
System Radius (mm)	60
Lens Index	1.41
Lens Diameter (mm)	2
Lens Spacing (mm)	5.23
Lens curvature (radius mm)	1.3
Lens height (mm)	0.47
Distance to image plane (mm)	4
Central fiber core dia. (mm)	0.245
Cent. fiber clad dia	0.25
Off-Axis fiber core dia	0.245
Off-Axis fiber clad dia	0.25
Fiber NA (deg)	30.66
NA in lens (deg)	21.2

Design Specs	
Resolution	
Inter ommatidial angle (deg)	5
(overlap)	5.77
Central Field (deg)	4.95
Off-axis field (deg)	4.95
Hyperacuity	
Off-axis Field shift (deg)	0.062
Marginal focus (mm)	3.69
Full Fill B (bestfocus mm)	4.09
Paraxial focus (mm)	4.47